Ab initio investigation of point defects in bulk Si and Ge using a cluster method

Serdar Öğüt* and James R. Chelikowsky
Department of Chemical Engineering and Materials Science, Minnesota Supercomputing Institute, University of Minnesota, Minneapolis, Minnesota 55455-0132

(Received 14 June 2001; published 4 December 2001)

Atomic and electronic structures of various charge states $(2+,+,0,-,2-)$ of monovacancies V and divacancies V_2 in crystalline Si and Ge are calculated from first principles. The calculations are performed in real space on bulk-terminated spherical and prolate clusters that are passivated by hydrogens at the boundaries. Defect-induced Jahn-Teller distortions, Jahn-Teller and relaxation energies, vacancy wave function characters, and hyperfine parameters are calculated and compared with available experimental data. The magnitudes of Jahn-Teller distortions and energies are found to be smaller in Ge compared to Si for both V and V_2. Unlike in Si, the pairing type distortions induced by a divacancy in Ge are not large enough to result in a deep level crossing inside the band gap. Furthermore, the relaxed atomic configurations of the divacancy in Ge with resonant bond type distortions are found to be slightly lower in energy than those with pairing type distortions. The effect of the lattice constant at which the calculations are performed (experimental versus theoretical) is also examined, and found to be quite important, especially for Ge.

DOI: 10.1103/PhysRevB.64.245206 PACS number(s): 61.72.Ji, 71.55.Cn

I. INTRODUCTION

Point defects, such as monovacancies and divacancies, in the prototype elemental semiconductors have been the subject of many theoretical and experimental studies. Over the last three decades, researchers modeling such defects have had a variety of choices for their theoretical techniques.[1] In the 1970's, the cluster method, in which the bulk defect is simulated by a reasonably large cluster of atoms with a defect at the center,[2] was the most popular choice. Later, Green's function methods and more recently plane-wave supercell calculations within density functional theory became the favorite choices of theorists. In the last decade, advances in electronic structure algorithms, particularly the successful implementations of real space methods based on *ab initio* pseudopotentials,[3,4] have brought a new perspective in theoretical modeling of defects, namely the revival of cluster methods.

While the plane-wave supercell methods present a well-established technique with many advantages for investigating defect related properties (e.g., in calculating formation energies and defect concentrations), cluster methods can also offer an efficient and accurate approach for structural properties, especially within a real-space formalism. In particular, cluster calculations for charged defects can be implemented in a straightforward fashion without the need for a neutralizing background charge. Easy parallelizability of the algorithms that do not use fast Fourier transforms, and efficient diagonalization of sparse Hamiltonians, which need not be stored, are other important assets. As such, these advances have allowed us to perform *ab initio* cluster calculations of defects in semiconductors involving hundreds of atoms[5,6] and of optical gaps in Si quantum dots with more than 1000 atoms.[7] Another important feature of cluster methods for investigating point defects is related to the flexibility in choosing the system size that simulates the defect. In supercell calculations, the most common system sizes used for defect calculations are supercells with 64, 128, or 216 atoms. Large supercells model point defects reasonably well by minimizing the defect-defect interaction across the unit cells and the spurious dispersion of defect levels. Cluster calculations, on the other hand, eliminate defect-defect interactions, and the resulting defect-surface interactions are further minimized by appropriately passivating the surface. In addition, cluster methods present easy and efficient control of convergence for various physical properties by allowing intermediate system sizes. More importantly, the geometry of the clusters can be altered in such a way that the finite system mimics the bulk defect as closely as possible without making the number of atoms in the system prohibitively large. For example, if the defect-induced strains are only along a particular direction and otherwise decay rapidly away from it, it is important to include many shells of atoms along this particular direction. On the other hand, the inclusion of more atoms along other directions would unnecessarily increase the computational demand without bringing any significant physical difference. In this way, one can model point defects with anisotropic strain patterns by using effectively much larger system sizes than would be possible with conventional supercells or isotropic spherical systems.

In the last few years, we have successfully applied the cluster method to *ab initio* pseudopotential investigations of monovacancies (V) and divacancies (V_2) in crystalline Si.[5,6] In fact, the use of prolate clusters by identifying the relevant relaxation patterns as discussed above has helped greatly in understanding the structural and electronic properties of charged divacancies in crystalline Si, which were found to exhibit large pairing Jahn-Teller (JT) distortions. While point defects in Si have been investigated extensively both experimentally and theoretically with many different techniques, there have not been many studies on structural and electronic properties of defects in the other prototype group IV semiconductor, the isovalent Ge. In this paper, in addition to presenting more details about our work on V and V_2 in Si by also including different charge states, we make a comparative study of the same point defects in Ge with Si. We find

that the relaxation magnitudes associated with both V and V_2 in Ge are more strongly dependent on the lattice parameter at which the calculations are performed. At the experimental lattice constant, we observe that both the magnitudes and the physical ranges of the relaxations in Ge are smaller than in Si, with smaller JT distortions and energies. As a result, for the case of V_2, we find that relaxed structures of Ge with pairing type distortions do not exhibit a deep level crossing. In fact, such relaxed structures of V_2 in Ge with small pairing JT distortions are more likely to correspond to local minima, as they are found to be slightly higher in energy than those with resonant bond type distortions.

In Sec. II, we discuss the computational details of our work based on the real space higher-order finite-difference pseudopotential method and a cluster approach for modeling defects. In Sec. III, we examine the electronic and structural properties of monovacancies in bulk Si and Ge, commenting on the similarities and differences between the two group IV semiconductors, and the effect of the lattice parameter at which the calculations are performed. Atomic relaxations, wave function characters, Jahn-Teller energies, and hyperfine parameters associated with neutral and charged divacancies in Si and Ge are discussed in Sect. IV. Our results are finally summarized in Sec. V.

II. COMPUTATIONAL METHODS

Our calculations were performed using a cluster method. The bulk defects were simulated by bulk-terminated spherical and prolate Si and Ge clusters, which were passivated by hydrogens at the boundaries. For the case of the monovacancy V, the origins of the clusters were taken to be at the vacant site while for the divacancy V_2, the origins were taken to be at the midpoint of the line connecting the two vacant sites. Most of the clusters considered were terminated from the bulk spherically with complete shells $N_{sh}=4$ to 17 around the point defect. In order to take into account the anisotropic and long-ranged nature of the defect-induced relaxations without making the number of atoms too large, we also considered prolate clusters $X_{230}H_{180}$ for V, and $X_{246}H_{186}$ for V_2 (where X denotes Si or Ge), as shown in Fig. 1. These clusters have incomplete shells which include atoms only along directions with the largest atomic relaxations. As will be discussed in the next section, the largest JT distortions for V^-, V^0, and V^+ occur along the two perpendicular directions $[110]$ and $[1\bar{1}0]$ containing the vacant site. The prolate cluster $X_{230}H_{180}$ is generated from the $X_{190}H_{148}$ cluster by adding atoms along these zigzag chains. Similarly, the prolate $X_{246}H_{186}$ cluster for simulating V_2 is built on top of the base $X_{206}H_{158}$ cluster with atoms added along the zigzag chains of atoms in the $[1\bar{1}0]$ direction containing the vacant sites. For each cluster, only X atoms fully coordinated with other X atoms were relaxed. The atomic compositions, sizes, and the number of relaxed atoms for all clusters considered for V and V_2 are given in Table I.

Electronic structure calculations within the framework of density functional theory were carried out in real space using the *ab initio* higher-order finite difference pseudopotential method.[3] This method, which does not require the use of fast-Fourier transforms and results in sparse Hamiltonian matrices that need not be stored, has an easily parallelizable algorithm capable of handling several hundred atom systems in a straightforward fashion on parallel computers. We used Troullier-Martins pseudopotentials in nonlocal and local forms for X and H, respectively.[8] The calculations were performed within the local density approximation (LDA) using the exchange-correlation functional of Ceperley and Alder.[9] We used grid spacings of $h=0.75$ and 0.6 a.u. for Si and Ge, respectively. We carefully checked the convergence of the physical results by reducing h down to 0.6 a.u. (Si) and 0.45 a.u. (Ge), upon which no significant changes on the relaxed structures were observed. The kinetic energy in the finite difference expression was expanded to twelfth order in h. We used zero boundary condition for the wavefunctions by requiring them to vanish outside a spherical domain, which was 6.5–7.5 a.u. away from the last shell of X atoms. The Hartree potential was solved by discretizing the Poisson

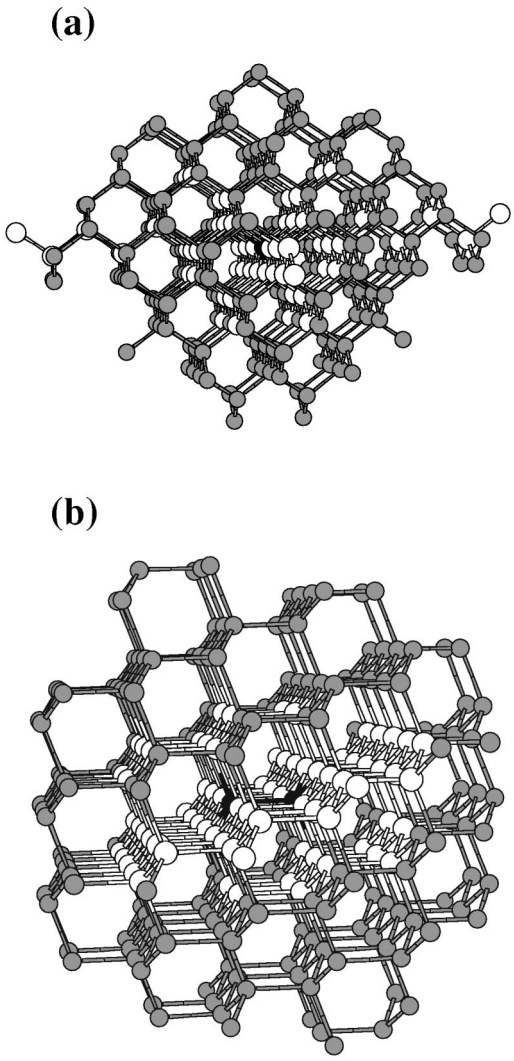

FIG. 1. Atomic structures of prolate clusters (a) $X_{230}H_{180}$, (b) $X_{246}H_{186}$, used for modeling the monovacancy and divacancy, respectively. H atoms are not shown. The black balls correspond to the vacant sites. The highlighted atoms (in white) correspond to atoms which undergo significant distortions due to the defect.

TABLE I. Sizes of H-passivated clusters (X=Si or Ge) used for simulating the monovacancy V and divacancy V_2 given in terms of the number of X shells N_{sh}, atomic composition, and diameters d. Diameters are given for Si, and can be scaled with the lattice constant ratio to calculate them for Ge. Also given are the number of relaxed X atoms N_{re} for each cluster. For the prolate $X_{230}H_{180}$ and $X_{246}H_{186}$ clusters, the dimensions refer to the smallest and largest values along different directions.

Defect	N_{sh}	Composition	d (Å)	N_{re}
V	4	$X_{34}H_{36}$	10.9	4
	5	$X_{46}H_{60}$	11.8	16
	6	$X_{70}H_{84}$	13.3	28
	7	$X_{86}H_{76}$	14.1	34
	8	$X_{98}H_{100}$	15.4	46
	9	$X_{122}H_{100}$	16.1	58
	12	$X_{166}H_{124}$	18.8	86
	13	$X_{190}H_{148}$	19.4	98
	13–25	$X_{230}H_{180}$	19.4–27.0	114
V_2	4	$X_{36}H_{42}$	11.1	6
	7	$X_{84}H_{78}$	14.5	30
	9	$X_{128}H_{98}$	16.5	60
	11	$X_{164}H_{122}$	18.2	78
	13	$X_{206}H_{158}$	19.7	114
	17	$X_{316}H_{198}$	22.5	188
	13–25	$X_{246}H_{186}$	19.7–27.2	138

equation and matching the boundary potential to a multipole expansion of the charge density with angular momentum $l=9$ to 20. The above grid spacings and boundary sphere dimensions resulted in Hamiltonian matrices of up to $\sim$320 000(Si) and 625 000 (Ge) for the case of prolate clusters. The Hamiltonians were diagonalized for self-consistent solutions of up to $\sim$750 eigenpairs (for $X_{316}H_{198}$) using a generalized Davidson algorithm[10] with dynamical residual tolerance. The relaxed geometries for each charge state were found without imposing any symmetry constraint using the initially scaled variable metric minimization scheme of Broyden, Fletcher, Goldfarb, and Shanno.[11] While small cluster calculations were performed sequentially on Cray C-90 and IBM SP2, large-scale calculations were run in parallel on the T3E and SP2 using a domain decomposition approach by mapping portions of the entire physical space onto each processor.[12]

III. MONOVACANCIES IN SILICON AND GERMANIUM

The ideal monovacancy in both Si and Ge induces a nondegenerate a_1 level in the valence band manifold and a triply degenerate t_2 deep level inside the band gap. This t_2 level accommodates three, two, one, and zero electrons for the charge states of V^-, V^0, V^+, and V^{2+}, respectively. Therefore, except for V^{2+} the lattice should distort to remove the degeneracy associated with the highest occupied state, thereby gaining electronic energy.[13] In our calculations, we find that for V^+ and V^0, the JT distortion reduces the ideal T_d symmetry to D_{2d} with the lowest deep level occupied with one or two electrons, respectively, while the unoccupied level remains doubly degenerate. In terms of atomic relaxations of the four atoms in the first shell, this distortion can be viewed as two pairs being pulled toward each other to form weak covalent bonds on top of radial (breathing mode) relaxations. For V^-, the extra electron in the previously degenerate e level causes yet another JT splitting. As a result, we find that one of the two pairs in the first shell gets pulled toward each other slightly more than the other resulting in a C_{2h} symmetry. Finally, for V^{2+} for which the highest occupied state is at the valence band maximum and the deep levels in the gap are fully unoccupied, we observe purely breathing mode distortions (i.e., no JT distortions).

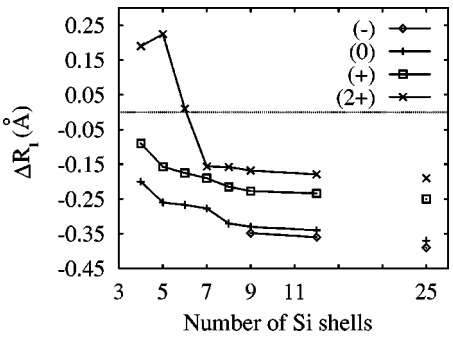

FIG. 2. Relaxation magnitudes (in Å) of the first shell atoms as a function of the cluster size (given in terms of the number of Si shells N_{sh}) for $V^-(\diamond), V^0(+), V^+(\square)$, and $V^{++}(\times)$ in Si. Negative sign means inward relaxation. The unconnected data points at $N_{sh}=25$ refer to values for the $Si_{230}H_{180}$ cluster.

Figure 2 shows the magnitudes of the relaxations of the first shell atoms for various charge states of Si as a function of the cluster size. In agreement with recent calculations,[14–18] we find inward relaxation of the atoms for all charge states for large enough system sizes. The magnitude of the relaxations increases as the charge state changes from $(2+)$ to $(-)$. This can be understood in terms of the strengthening of the weak covalent bonds between the first shell of atoms upon addition of extra electrons. The size of the cluster plays an important role in determining the magnitudes and signs of the relaxations. For example, for the three smallest clusters $Si_{34}H_{36}$, $Si_{46}H_{60}$, and $Si_{70}H_{84}$ the relaxations in V^{2+} are found to be outward, in agreement with recent supercell calculations.[18] Similar outward relaxations are also observed for V^{2+} in Ge when small clusters are used. Table II shows the interatomic distances for the first shell atoms in relaxed Si and Ge monovacancies for various charge states.

When the calculations are performed at the experimental lattice constants of Si (5.43 Å) and Ge (5.66 Å), we observe that the magnitudes of the relaxations in the first and higher shells are larger in Si than in Ge. This is in agreement with recent calculations of Fazzio *et al.*[19] who found smaller vacancy-induced distortions in Ge compared to Si. The general pattern of the relaxations can be described as an anisotropic propagation along the zigzag chains of atoms in the perpendicular [110] and $[1\bar{1}0]$ directions that contain the vacant site. Figure 3 shows the significant distortion amplitudes as a function of the shell index for V^0 in Si and Ge.

TABLE II. Calculated interatomic distances and Jahn-Teller energies for relaxed monovacancies of Si and Ge in various charge states. d_{p_1} and d_{p_2} denote the distances between the paired atoms, and d_{12} denotes the distances between atoms of different pairs. All distances are in Å, all energies are in eV.

Defect	d_{p_1}	d_{p_2}	d_{12}	E_{JT}
Si V^{2+}	3.54	3.54	3.54	
Si V^{+}	3.38	3.38	3.53	0.05
Si V^{0}	3.09	3.09	3.46	0.32
Si V^{-}	3.02	3.14	3.36	0.29
Ge V^{2+}	3.75	3.75	3.75	
Ge V^{+}	3.72	3.72	3.99	0.02
Ge V^{0}	3.53	3.53	3.89	0.12
Ge V^{-}	3.36	3.52	3.72	0.08

The shown amplitudes correspond to the highlighted atoms in Fig. 1(a) manifesting the degree of anisotropy in the propagation of the distortions. For the case of Si [Fig. 3(a)], the largest relaxations start from ≈ 0.38 Å in the first shell and decay slowly to 0.07 Å in the eighteenth shell. The shell indices with the largest relaxations (first, second, fifth,eighth, thirteenth, and eighteenth) correspond to the zigzag chains of atoms passing through the vacant site in the [110] and $[1\bar{1}0]$ directions. The distortions of the atoms along these two chains are almost parallel to the chain directions with atoms

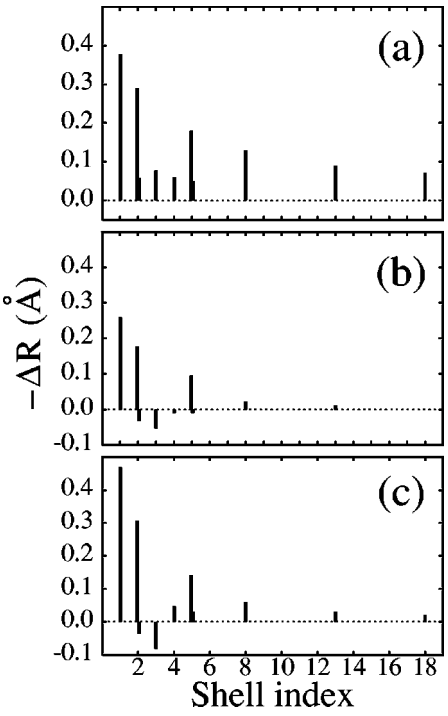

FIG. 3. Distortion amplitudes (in Å) as a function of the shell index for (a) V^0 in Si, (b) V^0 in Ge at the experimental lattice constant of 5.66 Å, (c) V^0 in Ge at the LDA lattice constant of 5.59 Å. Only distortions with $|\Delta R| > 0.05$ Å are shown in (a). The long-ranged distortion amplitudes extending to the eighteenth shell in (a) correspond to atoms in the [110] and $[1\bar{1}0]$ zigzag chains containing the vacant site.

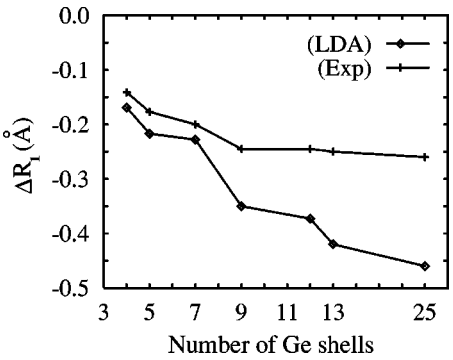

FIG. 4. Relaxation magnitudes (in Å) of the first shell atoms as a function of the cluster size (given in terms of the number of Ge shells N_{sh}) for V^0 in Ge when the calculations are performed at the experimental (+) and LDA ($\diamond$) lattice constants. $N_{sh}=25$ refers to the $Ge_{230}H_{180}$ cluster.

in the same chain and shell relaxing toward each other. Going away from these two particular chains in either [110], $[1\bar{1}0]$, or [001] directions, the relaxation decay quite rapidly.

For the case of Ge, on the other hand, the magnitudes of the relaxations (when the calculations are performed at the experimental lattice constant) are not only smaller compared to Si, but also decay more rapidly along all directions including the two particular zigzag chains. For example, as shown in Fig. 3(b), the distortion amplitudes in the first shell are only 0.25 Å, and decay to 0.02 Å in the eighth shell. In addition to the small and relatively short-ranged relaxations in Ge, the sign of the distortions are also different in various shells with some atoms relaxing away from the vacancy.

While the theoretical lattice constant of Si is found to be only 0.1% smaller than the experimental value, it is underestimated by 1.2% for Ge in our LDA calculations. In investigations of defects within first principles approaches, there is no general consensus as to whether the experimental or the theoretically calculated lattice constant should be used in the calculations. While we believe this usually does not make a significant difference in calculations of the physical observables (since either the discrepancy between theory and experiment is very small, or the results are insensitive to the lattice constant used), we observe that in some cases such as Ge, the lattice constant has a substantial effect in the magnitude of the distortions and structural energetics.

When the calculations are performed at the theoretical lattice constant of 5.59 Å for Ge, we find that the relaxations of the atoms are significantly larger than those calculated at the experimental lattice constant. As shown in Fig. 3(c), the distortion amplitudes in the first shell are ≈ 0.48 Å, which are even larger than those of Si. On the other hand, the relaxations still decay more rapidly compared to Si. This behavior of substantially larger distortions at the theoretical lattice constant is more pronounced as the size of the system is increased. Figure 4 shows the magnitude of the relaxations in the first shell around the neutral Ge monovacancy as a function of the system size for the cases of experimental and theoretical lattice constants. The significant increases in the magnitudes of the first shell relaxations that occur in the nine, thirteen, and eighteen shell clusters are due to the fact

that these clusters allow the relaxations of extra shells of atoms along the zigzag chains containing the vacant sites.

The increase in the magnitude of the JT distortions when the lattice is contracted is also observed for Si. For example, our calculations for the $Si_{122}H_{100}$ cluster find that the magnitude of the distortions in the first shell $|\Delta R_1| = 0.33$ Å at the experimental lattice constant $a_{\rm exp}$ increases to 0.37 and 0.45 Å at $a = 0.99a_{\rm exp}$ and $0.98a_{\rm exp}$, respectively. Such increases in the magnitude of the distortions are not too surprising, as the decrease in the lattice constant makes it easier for stronger covalent bonds to be formed between the pairs of atoms in the first shell at a slightly lower expense of weakening their back bonds. A similar version of the above observations has already been reported in the literature by Antonelli, Kaxiras, and Chadi regarding the effects of pressure on the structure of the Si monovacancy.[17] These authors found two distinct distortions associated with V^0 in Si, one of which exhibited much larger JT distortions, but was an unstable equilibrium configuration at zero pressure. At finite pressures the authors suggested that this structure of the monovacancy with larger JT distortions should become dominant. Since the effect of the pressure is to reduce the lattice constant, these earlier results are in agreement with our present calculations for Si and Ge.

Regarding structural energetics, the calculated Jahn-Teller energies $E_{\rm JT}$ (energy difference between the fully relaxed structures and those relaxed with a constrained T_d symmetry) are also given in Table II. The calculated $E_{\rm JT}$ of 0.05, 0.32, and 0.29 eV for the Si monovacancy in charge states of $(+)$, (0), and $(-)$, respectively, do not seem to be in good agreement with the experimental estimates of 0.4, 1.5, and 2.1 eV. We believe that while the size of the system might play a minor role, the major source of the discrepancy has to do with the tendency to overestimate the experimental $E_{\rm JT}$. This tendency is greatly increased when the strain has a long-ranged character, since the externally applied uniform stress assists in the motion of all atoms involved (especially in the vacancy-containing zigzag chains along [110] and $[1\bar{1}0]$). Since $E_{\rm JT}$ estimates come from projecting out only the stress components for the first shell atoms, one might expect a large difference between the experimental and theoretical Jahn-Teller energies for systems with long-ranged distortions.[20] On the other hand, we expect that our values should be slightly larger than the reorientation barriers between symmetry-equivalent distortions, and we find this to be the case as the experimental estimates of the reorientation energies in Si are 0.013, 0.23, and 0.08 eV for V^+, V^0, and, V^-, respectively. For Ge, which exhibits smaller JT distortions, we find, as expected, smaller $E_{\rm JT}$ values of 0.02, 0.12, 0.08 eV for the $(+)$, (0), and $(-)$ charge states, respectively. When the calculations are performed at the theoretical lattice constant of Ge, the calculated Jahn-Teller energies are found to be larger than those calculated at $a_{\rm exp}$, e.g., $E_{\rm JT}$ increases to 0.22 eV for the neutral monovacancy.

IV. DIVACANCIES IN SILICON AND GERMANIUM

Removing two adjacent atoms from a perfect group IV semiconductor creates a simple divacancy V_2. In its ideal (undistorted) structure, this results in a lattice with a D_{3d} symmetry. The divacancy-induced defect levels are the a_{1u} and a_{1g} levels inside the valence band manifold and the two doubly degenerate ones, labeled e_u and e_g, inside the band gap. From electron counts associated with six dangling bonds, the gap levels can accommodate one, two, and three electrons for charge states V_2^+, V_2^0, and V_2^-, respectively. Since the (lower) e_u level can accommodate up to four electrons, it implies that for the relaxed structure, the e levels will split as a result of a JT distortion which lowers the symmetry and helps gain electronic energy. When the symmetry is lowered to C_{2h}, each e level splits into a and b, producing the four levels a_g, a_u, b_g, and b_u. Of these, a_g and b_u have amplitudes, and b_g and a_u have nodes on the mirror plane of the C_{2h} distortion. This plane is the one that contains the vacant sites and atoms 3 and 6 in Fig. 5(a). The important feature in understanding the electronic structure of the simple divacancy in Si and Ge is related to the relative ordering of these levels, which is determined by both the sense and the magnitude of the distortion.

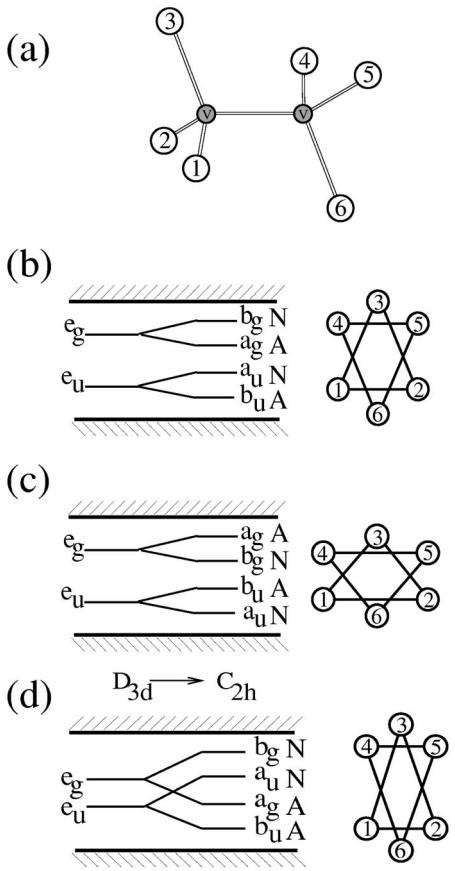

FIG. 5. (a) Atomic structure of V_2 with its six nearest neighbor atoms. The small shaded circles labeled by *V* represent the vacant sites. (b)–(d) Electronic structures, level symmetries, and the corresponding atomic structures viewed along the [111] divacancy axis for the cases of (b) small pairing Jahn-Teller distortion, (c) resonant bond configuration, and (d) large pairing Jahn-Teller distortion. The letters A and N next to the level symmetries represent whether the level has amplitude or node, respectively, on the mirror plane of the C_{2h} distortion.

With respect to the sense of the C_{2h} distortion, there are two different ways in which the first shell of atoms around the divacancy can move. They can relax either in a pairing sense [Fig. 5(b)], where atoms 1 and 2 are pulled toward each other such that $d_{12}<d_{13}=d_{23}$(d_{ij} being the distance between atoms i and j), or in a so-called resonant bond (RB) configuration [Fig. 5(c)] where $d_{12}>d_{13}=d_{23}$. As illustrated in Fig. 5, the difference in the electronic structure for the two types of distortions is simply the reversal of the a and b levels split from both e_g and e_u levels. With respect to the magnitude of a particular (either pairing or RB) distortion, there are also different orderings of the four deep levels. For example, in the case of a small pairing JT distortion [Fig. 5(b)], the splittings of a and b from each e level are small, so that the a_g and a_u levels do not cross each other inside the gap. Upon increasing the degree of the pairing distortion [Fig. 5(d)], it is possible for the upper a_g level to dip below the a_u level (and even below the b_u level for much larger distortions). Similar situations exist for the case of the RB distortions.

The importance of these level orderings inside the band gap can be recognized when one considers the wave function characters (particularly the presence of a node or amplitude on the mirror plane) of the highest occupied state. Electron paramagnetic resonance (EPR) experiments, which can identify the node versus amplitude character of the unpaired electron on the mirror plane, help determine the possible atomic structures of various charge states of V_2. This was certainly the case for determining the electronic and atomic structures of the divacancy in Si.

A. Silicon

1. Experimental and theoretical findings

The pioneering EPR experiments of Watkins and Corbett from nearly 35 years ago[21] established that for both $(+)$ and $(-)$ charge states of the divacancy in Si, the lattices have the low the symmetry of C_{2h}. From stress-induced defect alignment studies, they determined that the C_{2h} distortion occurs in a pairing sense. In addition, they observed that the highest occupied states for both charge states have amplitudes on the mirror plane. The Jahn-Teller energies $E_{\rm JT}$ were estimated to be large, 1.3 and 2.4 eV for V_2^+ and V_2^-, respectively. From these, Watkins and Corbett concluded that the JT distortions associated with the divacancy in Si had to be large enough for the upper a_g level to dip below the a_u (or even b_u) levels, so that the observed wavefunction characters, the sense of the distortion, and magnitudes of $E_{\rm JT}$ could be accounted for. In this picture, the resulting electronic configurations would be $V_2^+:b_u^1$ (or a_g^1) and $V_2^-:b_u^2a_g^1$ (or $a_g^2b_u^1$). A small pairing JT distortion cannot be consistent with EPR experiments for V_2^-, since it would imply the $b_u^2a_u^1$ configuration which has its highest occupied level with a node character in the mirror plane of the C_{2h} distortion.

Theoretical studies up to recently were not in agreement with the picture that emerged from these experimental interpretations.[15,16,22–26] Most of these calculations were performed with plane waves using supercells of 64 atoms. For the case of V_2^-, Saito and Oshiyama found a RB type distortion,[23] such that the electronic configuration $V_2^-:a_u^2b_u^1$ would still explain the amplitude character of the highest occupied state on the mirror plane. For V_2^+, they found a structure with a small pairing JT distortion ($V_2^+:b_u^1$), which is again consistent with the experimental wavefunction character. Similarly, Seong, and Lewis reported a RB type distortion for V_2^0.[16] More recently, the 216-atom supercell calculations of Pesola *et al.* found lower symmetry structures of S_2 symmetry changing from more of a pairing type to more of a RB type distortion in going from V_2^+ to V_2^-.[26] The main disagreement of these theoretical calculations with the experimental interpretations of Watkins and Corbett had to do with the sense of the JT distortion. The experimental finding of a rebonding by pairs, which was supported by both the estimates of the JT energies and the wave function characters, did not seem to be confirmed by these calculations which created an interesting controversy with regard to the actual ground state structures of divacancies in Si.[24,25]

Our first principles calculations using a cluster method resolved this theoretical controversy, confirming at the same time the experimental interpretations of Watkins and Corbett.[6] The key aspect of our calculations is related to the nature of the atomic relaxations associated with divacancies in Si. It is important to recognize that although the wave functions corresponding to defect-induced states decay rapidly beyond the first-shell of atoms, atomic relaxations do not follow the same pattern. As such, a typical 64-atom supercell used in most calculations is *not* adequate to describe the long-ranged and anisotropic relaxations that we find to be associated with $(+),(0)$, and $(-)$ states of the Si divacancy.

2. Large pairing Jahn-Teller distortions

Table III lists the interatomic distances corresponding to the relaxed geometries of various charge states of V_2. For minimum-energy ground state structures with pairing distortions, the magnitudes of the relaxations are quite large ranging from 0.86 Å in V_2^+ to 1.08 Å in V_2^- for the paired atoms near the divacancy. Such large relaxations for both V_2^0 and V_2^- result in the upper a_g level to dip below the b_u level, so that the first two levels from the valence band maximum have amplitude characters on the mirror plane of the C_{2h} distortion. This is in agreement with the EPR experiments of Watkins and Corbett. For V_2^+, on the other hand, the level crossing between the a_g and a_u does not occur (the two levels are separated by ~ 1 mRy in energy for the largest cluster considered), however, since in this case only the lowest deep level is occupied ($V_2^+:b_u^1$), the amplitude character of the wavefunction is again in agreement with EPR experiments.

As mentioned above, the size of the system that simulates the bulk divacancy is very important in determining its correct electronic structure. As an example, let us consider the case of V_2^0. Even for systems as large as $Si_{128}H_{98}$ or $Si_{164}H_{122}$ (with 9 and 11 shells of atoms around the divacancy), the crossing between a_g and a_u levels is not observed for the relaxed structures. This does not mean that the pairing distortions in the first shell of atoms are small. As a matter of

TABLE III. Relaxed atomic geometries of V_2^+, V_2^0, V_2^-, and V_2^{2-} for Si and Ge. Atomic structure data for both pairing (P) and resonant bond (RB) distortions are given. d_{ij} is defined in the text with respect to Fig. 5, and d_{iv} is the distance of atom i to the nearest vacant site. θ is the angle subtended by d_{12} at the atomic site 3. All distances are in Å, and angles in degrees. In the unrelaxed (bulk) geometry, $\theta = 60°, d_{12} = d_{13} = 3.84$ Å, $d_{1v} = d_{3v} = 2.35$ Å for Si, and $d_{12} = d_{13} = 4.00$ Å, $d_{1v} = d_{3v} = 2.45$ for Ge.

Element	Charge	d_{12}	d_{13}	θ	d_{1v}	d_{3v}
Si (P)	(+)	2.98	3.43	51.6	1.97	2.20
Si (P)	(0)	2.85	3.37	50.1	1.92	2.15
Si (P)	(−)	2.76	3.30	49.1	1.89	2.10
Si (RB)	(+)	3.42	3.26	63.3	2.09	2.04
Si (RB)	(0)	3.40	3.14	65.5	2.03	1.98
Si (RB)	(−)	3.34	3.17	63.4	2.02	1.99
Si	(2−)	3.29	3.29	60.0	2.05	2.05
Ge (P)	(+)	3.68	3.83	57.4	2.28	2.35
Ge (P)	(0)	3.60	3.77	56.9	2.21	2.32
Ge (P)	(−)	3.57	3.71	57.6	2.19	2.27
Ge (RB)	(+)	4.00	3.49	69.9	2.37	2.05
Ge (RB)	(0)	3.94	3.42	70.3	2.32	2.03
Ge (RB)	(−)	3.88	3.42	69.0	2.29	2.02
Ge	(2−)	3.56	3.56	60.0	2.17	2.17

fact, as shown in Fig. 6, where the first shell interatomic distances are plotted as a function of the system size, the relaxations and the degree of the distortions are considerably large for these clusters. The first cluster in which the crossing between the a_g and a_u levels is observed for V_2^0 is the $Si_{206}H_{158}$ cluster with 13 shells of atoms around the divacancy. The distance between the paired atoms in the first shell of the relaxed system drops by about 0.1 Å for this cluster (Fig. 6). This is because increasing the system size from 11 to 13 shells allows us to relax an extra shell of atoms along the zigzag chain of atoms in the $[1\bar{1}0]$ direction. Upon increasing the system size by including incomplete shells up to 25 ($Si_{246}H_{186}$) the degree of the pairing distortions increases further. The increase in the pairing distortions upon

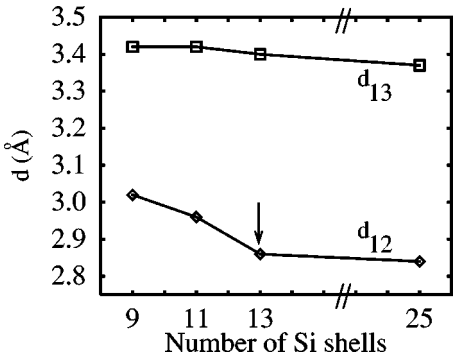

FIG. 6. First shell interatomic distances d_{12} and d_{13} (in Å) for V_2^0 in Si as a function of the cluster size. $N_{sh} = 25$ corresponds to the $Si_{246}H_{186}$ cluster. Note the sharp decrease in the distance between paired atoms, d_{12}, in going from $N_{sh} = 11 (Si_{164}H_{122})$ to $N_{sh} = 13 (Si_{206}H_{158})$.

going from $Si_{206}H_{158}$ to $Si_{246}H_{186}$ is actually more evident in the higher shells along the $[1\bar{1}0]$ direction as the magnitudes of relaxations increase by as much as 0.1 Å.

As a second example, let us consider the case of V_2^-. When this charge state of the divacancy is simulated with the $Si_{128}H_{98}$ cluster, the addition of the extra electron is still not enough to induce a crossing between the a_g and a_u levels, and the unpaired electron resides in the a_u level which has a node on the mirror plane. In fact, the extra electron reduces the pairing JT distortion making $d_{12} = 3.19$ Å. Furthermore, there is almost no energy gain in the system upon undergoing this JT distortion ($E_{JT} \approx 0$). If the extra electron is constrained to be in the amplitude state a_g resulting in the $b_u^2 a_u^0 a_g^1$ electronic configuration, the degree of the pairing JT distortion increases considerably with $d_{12} = 2.90$ Å. However, this configuration is 0.27 eV higher in energy than the structure with the small pairing JT distortion described above. These calculated values are in very good agreement with the 64-atom supercell calculations of Saito and Oshiyama.[25] Upon increasing the size of the system, the crossing between a_u and a_g levels in V_2^- is observed for $Si_{206}H_{158}$, and is further stabilized in the larger clusters.

3. General pattern of relaxations

When the divacancy axis is taken along the [111] direction, one can describe the general pattern of the relaxations as a long-ranged and anisotropic propagation along the zigzag chain of atoms in the $[1\bar{1}0]$ direction. On the other hand, the magnitudes of the relaxations decay quite rapidly in the [111] direction on either side of the divacancy, and along $[11\bar{2}]$ direction. In Fig. 1(b), the highlighted portion of the cluster corresponds to atoms which undergo significant distortions induced by the divacancy. The dimensions of this portion (containing 72 atoms) are 26.9 , 10.2 , and 6.6 Å, in the $[1\bar{1}0]$, [111], and $[11\bar{2}]$ directions, respectively. Such large variations along these perpendicular directions show the degree of the anisotropic relaxations associated with a divacancy in Si. The largest relaxations occur along the two zigzag chains, which contain the paired atoms (for example, atoms 1 and 2 in Fig. 5) and the vacant site nearest to them. As shown in Figs. 7(a) and 7(b) for V_2^- in Si, the inward pairing relaxations of atoms along these zigzag chains in the $[1\bar{1}0]$ direction are very large, and decay slowly from 0.53 Å in the first shell to as large as 0.07 Å in the eighteenth shell. The atoms in the same shell on opposite sides of the divacancy relax mainly toward each other. The two atoms not shown in Fig. 7(a), which also have large inward relaxations of 0.25 Å mainly along the $[11\bar{2}]$ direction, are in the first shell around the divacancy (atoms 3 and 6 in Fig. 5). As shown in Fig. 7(b), in going from the zigzag chain containing the vacant site to the next one in the [111] direction (half the atoms of which are bonded to the first zigzag chain), the magnitudes of the relaxations drop considerably. While almost all atoms relax inward, a few atoms such as the two atoms in the fourth shell relax outward.

The above observations suggest that the atomic relaxations induced by a divacancy with large pairing JT distor-

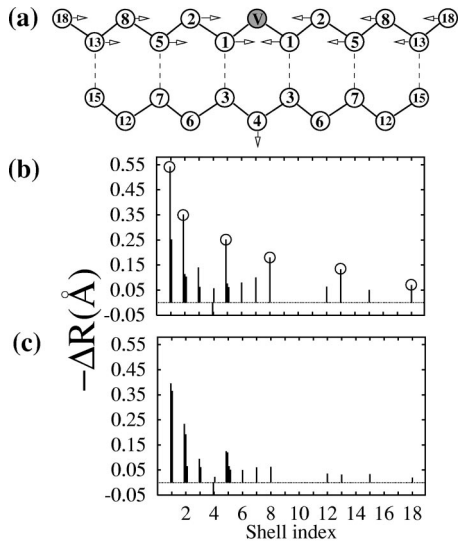

FIG. 7. (a) Two zigzag chains of atoms in the $[1\bar{1}0]$ direction (the upper containing one of the vacant sites labeled by *V*) along which the atoms relax considerably. The numbers labeling the atoms refer to the shell indices, not the atom indices in Fig. 5. The largest relaxations occur along the upper chain with the atoms in the same shell relaxing mainly toward each other as shown by the arrows on the atoms. Half the atoms in the lower chain are bonded to atoms in the upper chain as shown by dotted lines. These bonds are in the [111] direction parallel to the divacancy axis. (Hence, the two chains are *not* on the same plane). The arrow on the fourth shell atom in the lower chain indicates that the atom relaxes outward from the vacant site. (b) Distortion amplitudes (in Å) as a function of the shell index for V_2^- with large pairing distortions. Only displacements more than 0.05 Å are shown, corresponding mainly to the highlighted atoms in Fig. 1(b). The distortion amplitudes marked with circles refer to the upper chain of atoms containing the vacant site. (c) Same as in (b) for V_2^- with resonant bond distortions. Note the reduction in the magnitude of the relaxations compared to the case of large pairing distortions.

tions are long-ranged along the $[1\bar{1}0]$ direction, and decay rapidly along the two other perpendicular directions giving rise to quite an anisotropic relaxation pattern. As a result, a large and preferably anisotropic system is needed to simulate the divacancy in Si, so that all relevant propagation of atomic relaxations can be accommodated without making the number of atoms in the system too large. The prolate $Si_{246}H_{186}$ divacancy cluster is one such cluster generated from $Si_{206}H_{158}$ with atoms added along the zigzag chains in the $[1\bar{1}0]$ direction. Upon addition of atoms along the zigzag chain, the energetic stability of large pairing distortions are enhanced, and atomic relaxations in higher shells increase by as much as 0.1 Å.

We have also carefully investigated the structure of Si divacancy in its metastable RB configuration for all charge states. The calculated bond distances are also given in Table III. As shown in Fig. 7(c), the magnitudes of the relaxations in RB structures for the first shell (and subsequently higher shells) are not as large as in lower-energy structures with the large pairing distortions. For example, the inward relaxation of atoms 1 and 2 (Fig. 5) for RB distortions is only -0.36 Å, while that of atom 3 is -0.39 Å. Figure 7(c) also shows for V_2^- that the relaxations are not as long-ranged as in the large pairing distortion case.

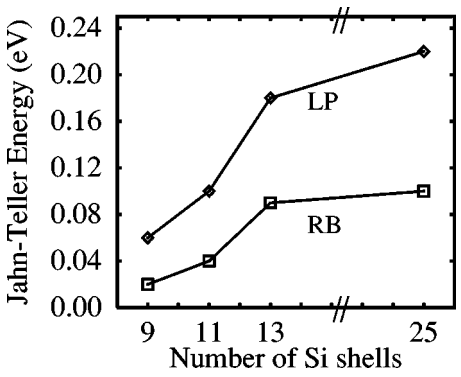

FIG. 8. Calculated Jahn-Teller energies of V_2^0 in Si as a function of cluster size (given in terms of N_{sh}) for large pairing (LP, ◇) and resonant bond (*RB*,□) distortions. $N_{sh}=25$ corresponds to the $Si_{246}H_{186}$ cluster.

4. Jahn-Teller energies

With respect to structural energetics, we find that the relaxation energies for the Si divacancy are 0.75, 1.1, 1.05, and 1.35 eV for charge states of $(+),(0),(-)$, and $(2-)$, respectively. These values are slightly larger than those reported in Ref. 26. For Jahn-Teller energies E_{JT}, we obtain values of 0.10 eV, 0.22 eV, and 0.15 eV for V_2^+, V_2^0, and V_2^-, respectively. The JT energies are strongly dependent on the system size, as expected, due to the long-ranged nature of the relaxations. Figure 8 shows the size dependence of E_{JT} for the neutral divacancy in Si for structures with large pairing and RB distortions. As the size of the system is increased from 9 shells to the prolate cluster with 25 incomplete shells, the relative stability of the structures with large pairing distortions over RB distortions increases from 0.03 to 0.12 eV. For the charge states of $(+)$ and $(-)$, we find that the structures with large pairing distortions are more stable than those with RB distortions by 0.05 and 0.12 eV, respectively.

The calculated E_{JT} for $(+)$ and $(-)$ charge states are smaller than the experimental values of 1.3 and 2.4 eV. In analogy with the monovacancy, a minor source of the discrepancy between the experimental estimates and the theoretical values can be attributed to the size of the system. However, the main reason for the discrepancy should be the overestimate of experimental values arising from the long-ranged character of the relaxations as discussed in the previous section. This latter observation actually helps understand the structural energetics of divacancies in Si by offering a physical interpretation of experimental estimates of JT and reorientation barrier energies and theoretical values. Upon removing two atoms from a perfect Si lattice, each of six neighboring atoms around the divacancy is left with one dangling bond. Naturally, this is not an energetically very favorable configuration, and the atoms try to form at least weak covalent bonds with each other. In the structures with large pairing distortions, the paired atoms manage to do this by forming relatively strong covalent bonds (compared to the

undistorted case) by moving toward each other by as much as 1.1 Å, resulting in a Si-Si bond distance near 2.80 Å. This distance is only 20% larger than the ideal Si bondlength, indicating the strength of the created bond. If one were to focus just on this aspect of effectively eliminating the dangling bonds in the first shell, a quite large stabilization energy would be obtained. However, when the paired atoms move by such large amounts to form covalent bonds, this results in stretching of the back bonds mainly along the $[1\bar{1}0]$ direction which is energetically costly. As a result, the strain goes out to large distances minimizing the cost of distorting the lattice. In a sense, the JT stabilization energy emerges from two competing phenomena: the energy gain from forming the relatively strong covalent bonds between dangling atoms of the first shell at the expense of creating a long-ranged strain to sustain the strong covalency.

The above observations suggest that the large experimental estimates for E_{JT} are due to the particular atomic relaxation patterns of the divacancy. As a matter of fact, the large differences between the estimated E_{JT} [1.3 and 2.4 eV for $(+)$ and $(-)$ charge states] and the reorientation barriers between symmetry-equivalent distortions [0.07 and 0.06 eV for $(+)$ and $(-)$ charge states] was a matter of controversy in establishing the sense of the JT distortions.[24,25] Our calculations are in good agreement with the above reorientation barriers assuming that in a simple $E\times e$ ''Mexican hat'' potential picture,[20,24,27] the reorientation barriers should correspond to the energy difference between the saddle point RB distortions and large pairing distortions, which are calculated to be 0.05 and 0.12 eV for $(+)$ and $(-)$ charge states, respectively. Finally, we note that another independent estimate of E_{JT} for the neutral divacancy comes from the 1.8 micron absorption band identified by Cheng *et al.* as coming from a filled pairing bond to the relatively unshifted spin orbitals.[28] In a simple degenerate perturbation theory, this absorption band should be approximately twice E_{JT} for V_2^0, giving an estimate of 0.34 eV, quite close to the calculated value of 0.22 eV.

5. Hyperfine coupling parameters

For additional comparisons with experimental results, we also calculated the hyperfine coupling parameters of V_2^+ and V_2^-. In order to overcome the complications associated with using pseudopotentials (i.e. the all-electron wavefunctions in the core region are not readily available), we adopted the scheme of Van de Walle and Blöchl.[29] The calculated isotropic hyperfine parameter a, anisotropic hyperfine parameter b, localization (η^2) and s component (α^2) amounts at the atomic sites in the first shell are given for both V_2^+ and V_2^- in Table IV along with the experimental data.[21,30] From the large (25–30 %) localization amounts η^2 and large isotropic hyperfine parameters a at the atomic sites 3 (or 6) for both charge states, we see that the wave function for the unpaired electron mainly resides at these sites. In general, we observe that the agreement between experimental and theoretical hyperfine coupling parameters and wavefunction characters for structures with the large pairing distortions is very good. Instead, our calculations for the isotropic hyperfine parameters of V_2^- with a relaxed RB distortion yield $a=289$ and 85 MHz at atomic sites 3 and 1, respectively, which are much too large compared to the experimental values of 195 and 32 MHz. These observations provide further evidence that the calculated structures with the large pairing distortions indeed correspond to the experimentally observed ground state structures.

TABLE IV. Hyperfine parameters (a and b), and wave function localization (η^2) and s component (α^2) amounts at the atomic sites in the first shell for V_2^+ and V_2^- with large pairing distortions. The values in parentheses are experimental data (Refs. 21,30).

Charge state	Atomic site	a (MHz)	b (MHz)	η^2 (%)	α^2 (%)
V_2^+	3	167.3 (147.7)	23.9 (27.7)	27.0 (27.7,31.0)	14.9 (11.7)
	1 or 2	31.4 (22.5)	1.2 (1.93)	2.0 (2.0)	39.5 (22.0,25.0)
V_2^-	3	239.5 (195.2)	17.2 (23.3)	22.1 (24.6,27.0)	25.8 (17.0)
	1 or 2	39.0 (31.5)	3.9 (2.2)	4.8 (3.0)	20.1 (25.6)

B. Germanium

The reduction in the magnitudes and spatial extents of the monovacancy-induced atomic relaxations in going from Si to Ge is also found for the case of divacancies. This observation has important consequences regarding the ordering of the divacancy-induced deep levels inside the band gap. As discussed at the beginning of this section, when the pairing JT distortions are small, the crossing between the a_g and a_u levels is not observed. We find this to be the case for all charge states of V_2 in Ge, resulting in electronic configurations for pairing distortions, $V_2^+ : b_u^1$ and $V_2^- : b_u^2 a_u^1$. More importantly, we find that the relaxed structures of V_2 in Ge with small pairing JT distortions have slightly higher ground state energies compared to structures with RB distortions.

Table III shows the interatomic distances corresponding to relaxed atomic configurations with small pairing JT distortions of various charge states of V_2 in Ge. Even in the $(-)$ charge state with the largest relaxations, the paired atoms get pulled toward each other by only 0.43 Å ($\approx$11% of the second-nearest neighbor distance), in comparison to 1.1Å found for Si. An indicator of the magnitude of the JT distortions is the deviation of the apex angle θ (subtended by d_{12} at the atomic site 3) from the bulk value of 60°. From examination of the θ values for Si and Ge divacancies with pairing type distortions, it is clear that the distortion magnitudes are much smaller in Ge compared to Si. Such small pairing type distortions in Ge cannot induce the level crossing observed in Si. In addition to the smaller magnitudes of pairing type distortions in Ge, the relaxations associated with V_2 are not as long-ranged as in Si. Figure 9(a) shows the

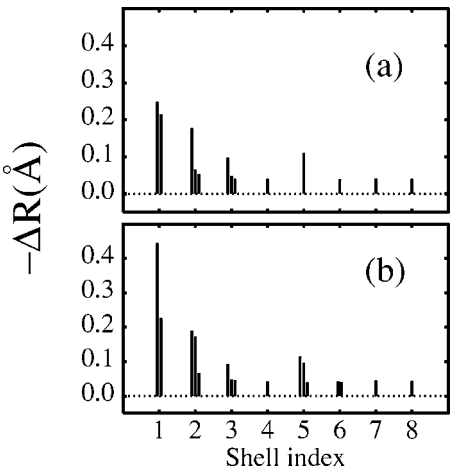

FIG. 9. Distortion amplitudes (in Å) as a function of the shell index for V_2^0 in Ge with (a) pairing, and (b) resonant bond distortions. Only distortions with $|\Delta R|>0.04$ Å are shown.

distortion amplitudes as a function of the shell index for significant distortions ($|\Delta R|>0.04$ Å) associated with V_2^0. All relaxations beyond the eighth shell are extremely small, and the long-ranged pattern along the two zigzag chains in the $[1\bar{1}0]$ direction found for the Si divacancy is practically not observed in Ge.

Another important difference in divacancy-induced distortions between Si and Ge is found when structures with RB type distortions are considered. The structural data for RB distortions in Ge are also shown in Table III. Interestingly, the values of θ indicate that the magnitudes of RB distortions are larger in Ge($\theta\approx 70°$) compared to Si($\theta\approx 64°$) for all charge states, unlike the case for pairing type distortions. Furthermore, the calculated distortion amplitudes [Fig. 9(b)] clearly indicate that Ge atoms in the first few shells around V_2 undergo much larger RB type relaxations in comparison to pairing type distortions. For example, the relaxations magnitudes $|\Delta R_1|$ for atoms in the first shell are 0.45 Å (two apex atoms) and 0.23 Å for RB distortions, while the calculated $|\Delta R_1|$ for pairing type distortions are 0.25 Å (two apex atoms) and 0.21 Å.

The relative decrease in the magnitude of pairing type JT distortions and the increase in the magnitude of RB distortions in going from Si to Ge suggest that the latter kind of distortions might lead to energetically more favorable structures for divacancies in Ge. We find this to be the case for all charge states of V_2 in Ge undergoing symmetry-lowering distortions. The calculated $E_{\rm JT}$ for RB type distortions are 0.09, 0.19, and 0.06 eV for $(+)$, (0), and $(-)$ charge states, respectively. However, the energy differences between relaxed structures with RB and pairing distortions are quite small. In all charge states, we find that RB structures are energetically more favorable by only ≈ 0.03 eV. We believe that such small energy differences calculated within LDA do not conclusively imply that the ground state structures of V_2 in Ge have RB distortions. More conclusive determination should come from EPR experiments, which can determine the node versus amplitude behavior on the mirror plane of the C_{2h} distortion.

It is also important to note that the relaxation patterns in RB type distortions are significantly different compared to pairing type distortions. In pairing distortions observed in Si, the formation of strong covalent bonds between the paired atoms creates a long-ranged propagation of relaxations along the zigzag chains in the $[1\bar{1}0]$ direction. For RB type distortions in Ge, the decomposition of the atomic displacements with respect to the three perpendicular directions $[1\bar{1}0]$, $[111]$, and $[11\bar{2}]$, shows that atoms in the first shell mainly relax in opposite senses along the $[11\bar{2}]$ direction: The apex atom (atom 3 in Fig. 5) and the two other atoms (atoms 1 and 2) move toward each other, resulting in resonant bonds between atoms 3 and 1, and atoms 3 and 2. This observation also offers a possible explanation of the change in the sense of the distortions for divacancies in Si and Ge. As discussed above, the formation of strong covalent bonds in the first shell of Si is favorable by a substantial amount (0.22 eV for V_2^0) in spite of the energetic cost of long-ranged strains along the zigzag chain. In the case of Ge, the energy gain from formation of covalent bonds becomes very comparable with the energy cost of long-ranged distortions. As a result, the atoms around a vacant site prefer to form two weak resonant bonds. These bonds should still be less energetically favorable compared to one strong covalent bond, but such a configuration does not require the energetically costly long-ranged strain associated with it.

When the divacancy calculations are performed at the theoretical lattice constant, we find that the magnitudes of the JT distortions (both pairing and RB type) in all charge states increase substantially, as in the case of the monovacancies. For example, for the case of pairing type distortions in V_2^0, the paired atoms get pulled toward each other by 0.85 Å (about 21% of the second nearest-neighbor distance) when the calculations are performed at the theoretical lattice constant. With $d_{12}=3.10$ Å and $d_{13}=3.51$ Å, this results in an apex angle of $\theta=52.5°$ indicating much larger relaxations and JT distortions. However, even in this case, the magnitudes of the distortions are not large enough for the level crossing to occur inside the band gap. Finally, performing the calculations at the theoretical lattice constant also increases the relative energetic stability of RB structures. For example, the calculated energy difference between RB and pairing type distortions increases from 0.03 to 0.09 eV for V_2^0.

V. SUMMARY

In this paper we have examined the structural and electronic properties of various charge states of monovacancies V and divacancies V_2 in bulk Si and Ge from first principles using a cluster method. For both V and V_2, the magnitudes and spatial extents of the relaxations, and the degree of the Jahn-Teller distortions are smaller in Ge compared to Si. For the Si divacancy, we find large pairing Jahn-Teller distortions in agreement with EPR experiments. The associated relaxations have an anisotropic and long-ranged character, which has made it difficult for theoretical structural determinations of the Si divacancy. For the Ge divacancy, we find that both pairing and resonant bond type Jahn-Teller distortions are

plausible candidates for ground state structures in all charge states, with resonant bond structures being energetically slightly more favorable. A conclusive determination of the sense of the distortion for Ge divacancies could come from future EPR experiments. Finally, we find that the lattice constant at which the LDA calculations are performed (experimental versus theoretical) could have an important effect on the structural and electronic properties of defects. We believe that it is important not to neglect this issue, and future studies examining the effect of pressure and lattice constant in defect calculations should prove quite useful.

ACKNOWLEDGMENTS

We would like to thank G. D. Watkins, H. Kim, J. D. Chadi, and C. Troparevsky for useful discussions. This work was supported by the National Science Foundation, U.S. Department of Energy under Grant No. DE-FG02-89ER45391, and the Minnesota Supercomputing Institute.

*Present address: University of Illinois at Chicago, Department of Physics (MC 273), 845 W. Taylor Street, Room 2236, Chicago, IL 60607-7059.

[1] S. T. Pantelides, in *Deep Centers in Semiconductors*, edited by S. T. Pantelides (Gordon and Breach Science Publishers, New York, 1986), p. 1.

[2] R.P. Messmer and G.D. Watkins, Phys. Rev. Lett. **25**, 656 (1970); Phys. Rev. B **7**, 2568 (1973).

[3] J. R. Chelikowsky, N. Troullier and Y. Saad, Phys. Rev. Lett. **72**, 1240 (1994).

[4] E.L. Briggs, D.J. Sullivan and J. Bernholc, Phys. Rev. B **52**, R5471 (1995); F. Gygi and G. Galli, *ibid.*, **52**, R2229 (1995); G. Zumbach, N.A. Modine and E. Kaxiras, Solid State Commun. **99**, 57 (1996).

[5] S. Öğüt, H. Kim and J.R. Chelikowsky, Phys. Rev. B **56**, R11353 (1997).

[6] S. Öğüt and J.R. Chelikowsky, Phys. Rev. Lett. **83**, 3852 (1999).

[7] S. Öğüt, J.R. Chelikowsky and S.G. Louie, Phys. Rev. Lett. **79**, 1770 (1997); J. R. Chelikowsky, S. Öğüt, and S.G. Louie, in *Proceedings of the Ninth CIMTEC–World Forum of New Materials*, ed. by P. Vincenzini and A. Esposti (Techna Srl, Faenza, 1999), p. 3.

[8] N. Troullier and J.L. Martins Phys. Rev. B **43**, 1993 (1991); L. Kleinman and D.M. Bylander, Phys. Rev. Lett. **48**, 1425 (1982).

[9] D.M. Ceperley and B.J. Alder, Phys. Rev. Lett. **45**, 566 (1980).

[10] Y. Saad, A. Stathopoulos, J. Chelikowsky, K. Wu, and, S. Öğüt, BIT **36**, 563 (1996).

[11] D.F. Shanno and K.-H. Phua, Math. Program. **14**, 149 (1978).

[12] A. Stathopoulos, S. Öğüt, Y. Saad, J.R. Chelikowsky and H. Kim, Comput. Sci. Eng. **2**, 19 (2000).

[13] G.D.Watkins, in *Deep Centers in Semiconductors* (Ref. 1), p. 147.

[14] A. Antonelli and J. Bernholc, Phys. Rev. B **40**, 10 643 (1989); E. Smargiassi, Mater. Sci. Forum **83-87**, 443 (1992); C.Z. Wang, C.T. Chan, and K.M. Ho, Phys. Rev. Lett. **66**, 189 (1991)); O. Sugino and A. Oshiyama, *ibid.* **68**, 1858 (1992).

[15] E.G. Song, E. Kim and Y.H. Lee, Phys. Rev. B **48**, 1486 (1993).

[16] H. Seong and L.J. Lewis, Phys. Rev. B **53**, 9791 (1996).

[17] A. Antonelli, E. Kaxiras and D.J. Chadi, Phys. Rev. Lett. **81**, 2088 (1998).

[18] M.J. Puska, S. Pöykkö, M. Pesola and R.M. Nieminen, Phys. Rev. B **58**, 1318 (1998).

[19] A. Fazzio, A Janotti, Antŏnio J.D. da Silva and R. Mota, Phys. Rev. B **61**, 2401 (2000).

[20] G.D. Watkins (private communication).

[21] G.D. Watkins and J.W. Corbett, Phys. Rev. **138**, A543 (1965); **138**, 555 (1965).

[22] O. Sugino and A. Oshiyama, Phys. Rev. B **42**, 11 869 (1990).

[23] M. Saito and A. Oshiyama, Phys. Rev. Lett. **73**, 866 (1994).

[24] G.D. Watkins, Phys. Rev. Lett. **74**, 4353 (1995).

[25] M. Saito and A. Oshiyama, Phys. Rev. Lett. **74**, 4354 (1995).

[26] M. Pesola, J. von Boehm, S. Pöykkö, and R.M. Nieminen, Phys. Rev. B **58**, 1106 (1998).

[27] M.D. Sturge, in *Solid State Physics*, edited by F. Seitz, D.Turnbull, and H. Ehrenreich (Academic Press, New York, 1967), Vol. 20, p. 92.

[28] L.J. Cheng, J.C. Corelli, J.W. Corbett and G.D. Watkins, Phys. Rev. **152**, 761 (1966).

[29] C.G. Van de Walle and P.E. Blöchl, Phys. Rev. B **47**, 4244 (1993).

[30] J.G. de Wit, E.G. Sieverts and C.A.J. Ammerlaan, Phys. Rev. B **14**, 3494 (1976); E.G. Sieverts, S.H. Muller, and C.A.J. Ammerlaan, *ibid.* **18**, 6834 (1978).